第18卷第5期
2003年9月

Vol.18, No.5
Sep., 2003

文章编号:1001—2060(2003)05—0482—04

闭式内可逆中冷回热布雷顿循环的功率优化

王文华, 陈林根, 孙丰瑞
(海军工程大学 核能科学与工程系, 湖北 武汉 430033)

摘 要:考虑高低温侧换热器、回热器和中冷器的热阻损失,以功率为优化目标,对恒温热源条件下内可逆闭式布雷顿循环的高低温侧换热器、回热器和中冷器的热导率以及中间压比的分配进行了优化。借助数值计算,分析了一些主要循环特征参数对最大功率及相应热导率和中间压比分配、双重最大功率的影响。

关 键 词:有限时间热力学;布雷顿循环;中冷回热;功率优化

中图分类号:TK121 文献标识码:A

1 前 言

自有限时间热力学理论产生以来,它在物理和工程领域的应用已取得了很大的进展[1~3]。利用此理论,国内外许多学者以不同的目标,如功率、效率、比功率、熵产率、生态学函数以及功率密度等,对布雷顿循环性能进行了分析和优化,并得到了很多有意义的结果[4]。这些工作主要研究了简单循环[5~11]、回热循环[12~13]和中冷循环[14]。本文建立了恒温热源条件下内可逆闭式燃气轮机中冷回热循环模型,考虑高低温侧换热器、回热器和中冷器的传热损失,以功率为优化目标,对高低温侧换热器、回热器和中冷器的热导率和中间压比同时进行了优化分配。通过数值计算,还给出了一些主要循环性能参数对最大功率及相应热导率和中间压比分配与总压比关系和双重最大功率的影响。

2 功率解析式

图1所示工作于恒温热源 T_H 和 T_L 间的闭式中冷回热布雷顿循环1—2—3—4—5—6—1。1—2为气体在低压压气机中的绝热压缩过程(压比为 π_1, 也称中间压比);2—3 为气体在中冷器中的冷却过程(中冷源温度为 T_I);3—4 为气体在高压压气机中的绝热压缩过程(压比为 π/π_1, 总压比为 π);4—7 为气体在回热器中的预热过程;7—5 为工质从高温热源吸热过程;5—6 为工质在涡轮中的绝热膨胀过程;6—8 为排气在回热器中的放热过程;8—1 为排气向低温热源的放热过程。

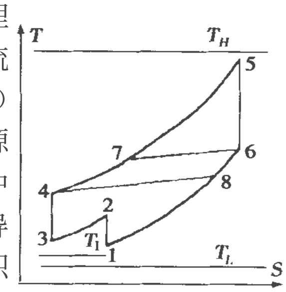

图1 循环 $T-S$ 图

设工质为定比热的理想气体,其热容率(质量流率 $\dot{m}$ 与定压比热 c_p 之积)为 C_{wf};工质与高低温热源间的换热器、回热器和中冷器均为逆流式,其热导率(传热系数与传热面积之积)分别为 U_H、U_L、U_R 和 U_I。由工质性质、热源与工质间的传热和换热器理论可知吸、放热率、回热流率和中冷热流率分别为:

$$Q_H = C_{wf}(T_5 - T_7) = U_H(T_5 - T_7)/ln[(T_H - T_7)/(T_H - T_5)] = C_{wf}E_H(T_H - T_7) \tag{1}$$

$$Q_L = C_{wf}(T_8 - T_1) = U_L(T_8 - T_1)/ln[(T_8 - T_L)/(T_1 - T_L)] = C_{wf}E_L(T_8 - T_L) \tag{2}$$

$$Q_R = C_{wf}(T_6 - T_8) = C_{wf}(T_7 - T_4) = C_{wf}E_R(T_6 - T_4) \tag{3}$$

$$Q_I = C_{wf}(T_2 - T_3) = U_I(T_3 - T_2)/ln(T_3 - T_I)(T_2 - T_I)] = C_{wf}E_I(T_2 - T_I) \tag{4}$$

其中:E_H、E_L、E_R、E_I 分别为高低温侧换热器、回热器和中冷器的有效度,

$$E_i = 1-\exp(-N_H),\ E_L = 1-\exp(-N_L),\ E_R = N_R/(N_R+1),\ E_I = 1-\exp(-N_I) \tag{5}$$

式中:N_H、N_L、N_R、N_I 分别为传热单元数,

$$N_H = U_H/C_{wf},\ N_L = U_L/C_{wf},\ N_R = U_R/C_{wf},\ N_I = U_I/C_{wf} \tag{6}$$

循环的功率 $P = Q_H - Q_L - Q_I$, 并定义无因次功率 $\overline{P} = P/(C_{wf}T_L)$, 则有:

收稿日期:2002—11—26
基金项目:全国优秀博士学位论文作者专项基金资助项目(200136);国家重点基础研究发展规划基金资助项目(G2000026301)
作者简介:王文华(1977—),男,湖北嘉鱼人,海军工程大学助教.

$$\overline{P}=[\{y^2(1-E_L)(1-E_I)E_R+y[(1-E_L)(1-2E_R)(1-E_I)-1]-(1-E_L)(1-E_R)(1-xE_I)+1\}E_H\tau_1+\{y^2[(1-E_R)E_H+E_R](1-E_I)+y[(1-E_H)(1-2E_R)(1-E_I)-(1-xE_I)]+(1-E_H)(1-xE_I)E_R\}E_L+\{y^2[(1-E_L)E_R+x^{-1}(1-E_R)E_H+x^{-1}E_LE_R]+y[(1-E_H)(1-2E_R)(1+x^{-1}E_L-E_L)-1]+(1-E_H)E_R\}E_I\tau_2]/\{y^2(1-E_L)(1-E_I)E_R+y[(1-E_H)(1-E_L)(1-2E_R)(1-E_I)-1]+(1-E_H)E_R\} \quad (7)$$

其中：$x=\pi_1^m$, $y=\pi^m$, $m=(k-1)/k$, k 为绝热指数，$\tau_1=T_H/T_L$ 为循环热温源比，$\tau_2=T_I/T_L$ 为中冷源与低温侧热源温比。

3　功率优化

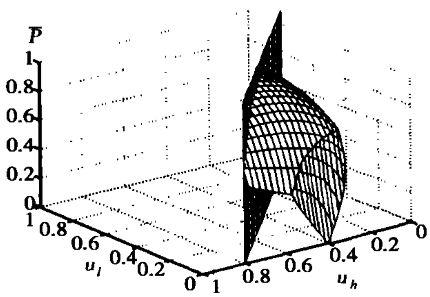

图 2　无因次功率与高低温侧热导率分配之间的关系（$u_i=0.2$）

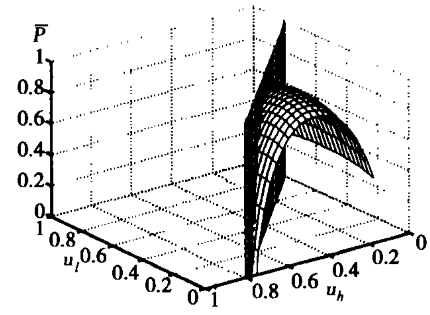

图 3　无因次功率与高低温侧热导率分配之间的关系（$u_r=0.2$）

由式(7)可知，对于给定的热源温比和总压比 π，无因次功率 $\overline{P}$ 是四个换热器的热导率和中间压比的函数。在一定条件下优选这些参数，可以优化循环功率。

当高低温侧换热器、回热器和中冷器的总热导率为定值，即 $U_H+U_L+U_R+U_I=U_T$ 时，定义热导率分配为：$u_h=U_H/U_T$, $u_l=U_L/U_T$, $u_i=U_I/U_T$, $u_r=1-u_h-u_l-u_i$，则有：

$$U_H=u_hU_T,\ U_L=u_lU_T,\ U_I=u_iU_T,$$
$$U_R=(1-u_h-u_l-u_i)U_T \quad (8)$$

另外，由实际情况还有下列约束：

$$0<u_h+u_l<1,\ 0<u_h+u_i<1,\ 0<u_l+u_i<1,\ 0<u_h+u_l+u_i<1, \quad (9)$$

热导率和中间压比的优化分配均由数值计算完成。计算时给定 $k=1.4$, $C_{wf}=1.0$ kW/K。

图 2 给出了 $U_T=5.0$ kW/K, $u_i=0.2$, $\pi=10$, $\pi_1=3$, $\tau_1=4.33$, $\tau_2=1$ 时，无因次功率($\overline{P}$)与高低温侧热导率分配(u_h, u_l)之间的三维关系；图 3 给出了 $U_T=5.0$ kW/K, $u_r=0.2$, $\pi=10$, $\pi_1=3$, $\tau_1=4.33$, $\tau_2=1$ 时，无因次功率($\overline{P}$)与高低温侧热导率分配(u_h, u_l)之间的三维关系；由图 2 发现，给定中冷器的热导率分配值，优化高低温侧换热器和回热器的热导率分配可有唯一的最佳功率；由图 3 发现，给定回热器的热导率分配值，优化高低温侧换热器和中冷器的热导率分配也有唯一的最佳功率；由此可知，给定总压比和中间压比时，同时对四个热导率优化，可得到循环的最优无因次功率($\overline{P}_{\rm opt}$)。图 4 给出了 $U_T=5.0$ kW/K, $\pi=10$, $\tau=1$ 时循环热源温比(τ_1)对最优

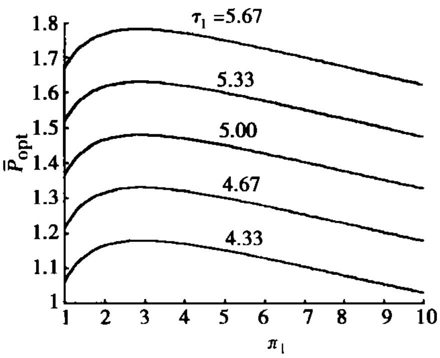

图 4　热源温比对循环最优功率—中间压比的影响)

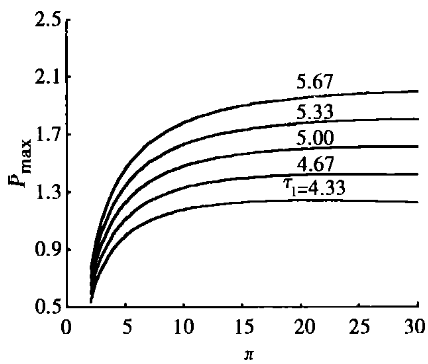

图 5　循环热源温比对最大功率—压比的影响

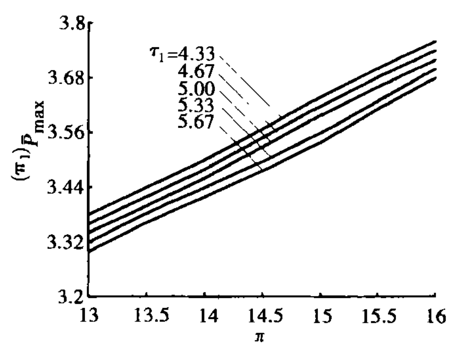

图 6　循环热源温比对最优中间压比—压比的影响

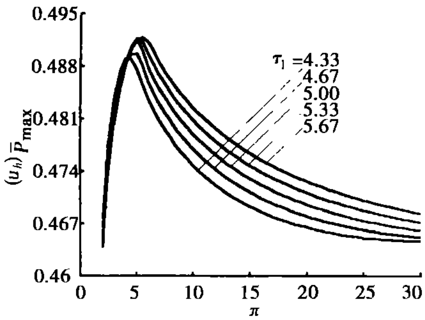

图 7　循环热源温比对高温侧最佳热导率分配—压比的影响

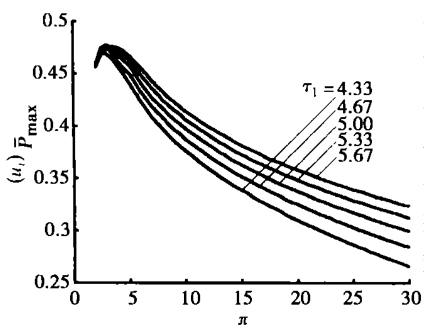

图 8　循环热源温比对高温侧最佳热导率分配—压比的影响

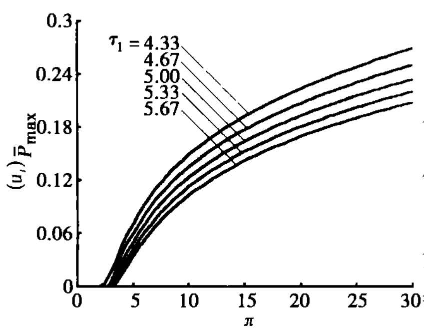

图 9　循环热源温比对中冷器最佳热导率分配—压比的影响

功率($\overline{P}_{opt}$)与中间压比关系的影响;从中可看出,最优功率($\overline{P}_{opt}$)与中间压比成类似抛物线关系,存在一个最优中间压比($(\pi_1)_{\overline{P}_{opt}}$)使最优功率($\overline{P}_{opt}$)取得最大值($\overline{P}_{max}$),即各抛物线的顶点。也就是说,对应一个最大功率,高低温侧换热器、回热器和中冷器存在一个唯一的最佳热导率分配($(u_h)_{\overline{P}_{max}}$、$(u_l)_{\overline{P}_{max}}$、$(u_r)_{\overline{P}_{max}}$、$(u_i)_{\overline{P}_{max}}$)和一个最佳的中间压比$(\pi_1)_{\overline{P}_{max}}$。

图5～图9分别给出了 U_T = 5.0 kW/K, τ_2 = 1 时循环热源温比(τ_1)对最大功率($\overline{P}_{max}$)及相应的中间压比($(\pi_1)_{\overline{P}_{max}}$)、高温侧换热器热导率($(u_h)_{\overline{P}_{max}}$)、低温侧换热器热导率($(u_l)_{\overline{P}_{max}}$)和中冷器热导率($(u_i)_{\overline{P}_{max}}$)与总压比($\pi$)关系的影响;图10～图14分别给出了 τ_1 = 4.33, τ_2 = 1 时总热导率(U_T)对最大功率($\overline{P}_{max}$)及相应的中间压比($(\pi_1)_{\overline{P}_{max}}$)、高温侧换热器热导率($(u_h)_{\overline{P}_{max}}$)、低温侧换热器热导率($(u_l)_{\overline{P}_{max}}$)和中冷器最佳热导率($(u_i)_{\overline{P}_{max}}$)与总压比($\pi$)关系的影响。

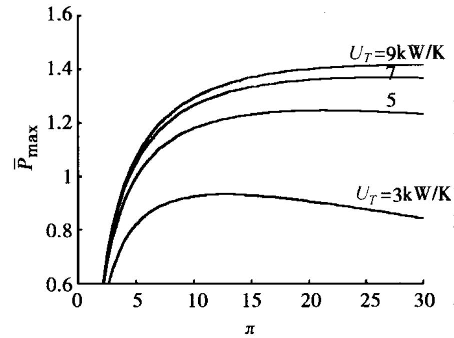

图 10　总热导率对最大功率—压比的影响

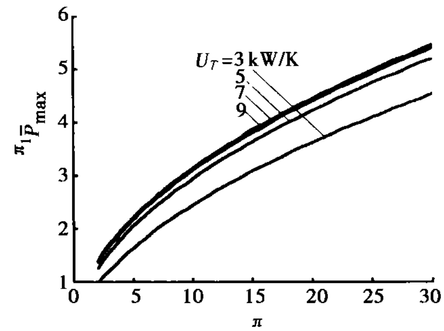

图 11　总热导率对最优中间夺比—压比的影响

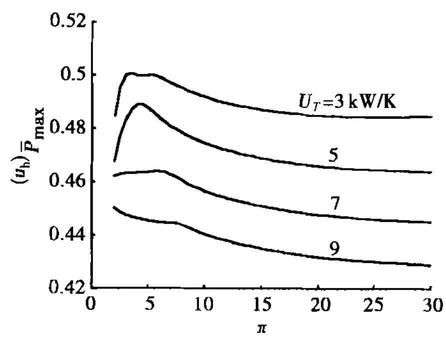

图 12　总热导率对高温侧最佳热导率分配—压比的影响

计算表明,循环最大功率随循环热源温比和总热导率的增大而增加,随中冷源与低温侧热源温比的增加而减小。从图10可知,随着总热导率的增大,其对最大功率的影响愈来愈小。最大功率与总压比成类似抛物线关系,这时存在一个最佳总压比$(\pi)_{\overline{P}_{max}}$使得最大功率取得双重最大值($(\overline{P}_{max})_{max}$),即图中各曲线极值点。计算表明,双重最大功率及相应的最佳总压比均随循环热源温比和总热导率增加而增大,随中冷源与低温侧热源温比增加而减小;如果总热导率增大到一定程度后继续增大,此时双重最大功率即相应的最佳总压比的变化就不太明显了。图15给出了循环热源温比(τ_1)和中冷源与低温侧热源温比(τ_2)对双重最大功率($(\overline{P}_{max})_{max}$)与总热导率($U_T$)关系的影响。计算还表明,最佳中间压比随总压比、中冷源与低温侧热源温比和总热导率单调增加,随循环热源温比单调减小。当总热导率增大到一定程度后,其对最佳中间压比影响甚微。高温侧换热器最佳热导率随总压比的增加,一般是先增加后

减小；随循环热源温比的增加呈先减小后增大的趋势，随中冷源与低温侧热源温比的增加单调递增，随总热导率的增加单调递减。低温侧换热器最佳热导率随循环热源温比的增加先减小后增大，随中冷源与低温侧热源温比的增加单调递增，随总热导率的增加单调递减。中冷器最佳热导率随循环热源温比和中冷源与低温侧热源温比的增加单调递减，随总热导率的增加单调递增。

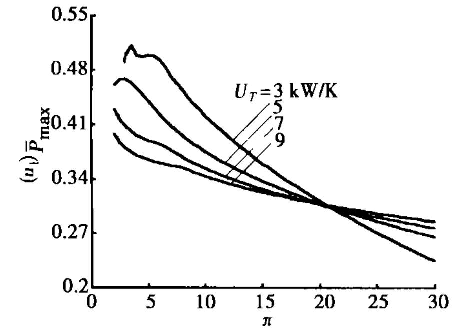

图 13　总热导率对低温侧最佳热导率分配—压比的影响

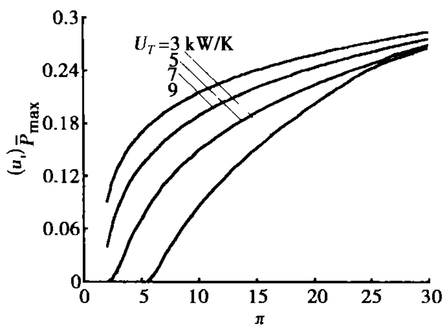

图 14　总热导率对中冷器最佳热导率分配—压比的影响

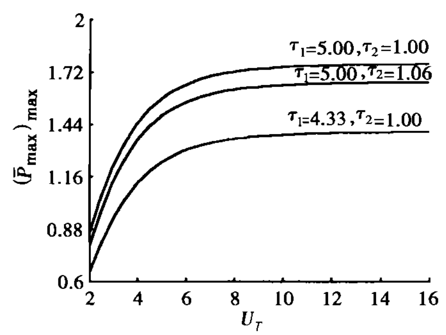

图 15　循环热源温比和中冷源与低温侧热源温比对双重最大功率—总热导率的影响

计算表明，当中冷源与低温侧热源温比过大或者总热导率过小时，在一定的总压比范围内，高低温侧换热器最佳热导率分配均为 0.5，亦即内可逆简单循环的输出功率最大。因此，中冷和回热过程的作用是否有利于增加功率输出，与其它参数的匹配选择有关。

4　结　论

用有限时间热力学方法对恒温热源条件下内可逆闭式中冷回热布雷顿循环的功率进行了优化分析，发现存在一个最佳的高低温侧换热器、回热器和中冷器的热导率和中间压比分配方案，使循环的输出功率达到最大；在此基础上，还存在一个最佳的总压比使得循环功率达到双重最大值（$(\bar{P}_{max})_{max}$）。由于热导率最优分配可以使给定循环功率条件下各换热器总尺寸最小化，因此本文的工作对提高动力装置性能有一定的指导作用。

参考文献：

[1]　BEJAN A. Advance engineering thermodynamics [M]. New York: Wiley, 1988.

[2]　BEJAN A. Entropy generation minimization: the new thermodynamics of finite-size devices and finite-time process [J]. **Appl Phys** 1996, **79**(3): 1191—1218.

[3]　CHEN L, WU C, SUN F. Finite time thermodynamic optimization or entropy generation minimization of energy systems[J]. **J Non—Equilib Thermodyn**, 1999, **24**(4): 327—359.

[4]　陈林根，吴　晏，孙丰瑞. 燃气轮机循环有限时间热力学分析：理论和应用[J]. 燃气轮机技术，2001, **14**(1): 46—53.

[5]　陈林根，孙丰瑞，陈文振. 闭式燃气轮机循环的最大功率输出[J]. 船舶工程，19**93**(4): 40—41.

[6]　IBRAHIM O M, KLEIN S A, MITCHELL J W. Optimum heat power cycles for specified boundary conditions [J]. **Trans ASME J Gas Turb Pow**, 1991, **113**(4): 514—521.

[7]　BEJAN A. Theory of heat transfer-irreversible power plants [J]. **Int J Heat Mass Transfer**, 1988, **31**(6): 1211—1219.

[8]　CHENG C Y, CHEN C K. Ecological optimization of an endoreversible Brayton cycle [J]. **Energy Convers Mgmt**, 1998, **39**(1/2): 33—44.

[9]　CHENG C Y, CHEN C K. Power optimization of an irreversible Brayton heat engine [J]. **Energy Sources** 1997, **19**: 461—474.

[10]　ZHENG J, CHEN L, SUN F, *et al*. Power density analysis of an endoreversible closed Brayton cycle [J]. **Int J Ambient Energy**, 2001, **22**(2): 95—104.

[11]　CHEN L, ZHENG J, SUN F, *et al*. Performance comparison of an endoreversible closed variable-temperature heat reservoir Brayton cycle under maximum power density and maximum power conditions [J]. **Energy Conversion and Management**, 2002, **43**(1): 33—43.

[12]　ROCO J M M, VELASCO S, MEDINA A, *et al*. Optimum performance of a regenerative Brayton thermal cycle [J]. **J Appl Phys**, 1997, **82**(6): 2735—2741.

[13]　CHEN L, ZHENG J, SUN F, *et al*. Power density analysis and optimization of a regenerated closed variable-temperature heat reservoir Brayton cycle [J]. **J Phys D: Appl Phys**, 2001, **34**(11): 1727—1739.

[14]　CHENG C Y, CHEN C K. Maximum power of an endoreversible intercooled Brayton cycle [J]. **Int J Energy Res** 2000, **24**(6): 485—494.

（辉　编辑）

增湿活化脱硫反应器内流动、蒸发与碰撞过程数值计算＝**Numerical Calculation of the Process of Flows, Evaporation and Collision in a Desulfurization Reactor Activated through Humidification** [刊,汉] / WU Shu-zhi, ZHAO Chang-sui, DUAN Yu-feng, et al (Education Ministry Key Laboratory on Clean Coal Power Generation and Combustion Technology under the Southeastern University, Nanjing, China, Post Code: 210096) //Journal of Engineering for Thermal Energy &Power. — 2003, 18(5). —471～474

Model study methods and numerical calculation results are described of the process in an activated (through spray water humidification) desulfurization reactor concerning the following: gas phase flows, water drop motion and evaporation, collision of water drops with particles of desulfurizing agents, as well as serous drops formed after the collision. The numerical simulation of a gas-phase turbulent flow model was conducted by the use of a k-ε dual-equation model. Water-drop motion and evaporation model was respectively simulated with the use of a random trajectory model and a water-drop evaporation model after a Ranz-Mashall modification. The collision between water drops and particles of desulfurizing agent was simulated by way of an inertia sedimentation model. The results of the numerical calculation indicate that the gas-phase velocity field in the activated reactor has evolved to a fully developed zone of turbulent flows. The atomized water drops injected into the reactor and the serous drops formed have completely evaporated within a short distance. The capture of desulfurizing agents mainly occurred in a section not far behind the location where water drops have been injected, followed by a drastic reduction of the capture efficiency. **Key words**: desulfurization, numerical simulation, evaporation, collision

介质特性对介质阻挡放电脱除 NO 影响试验研究＝**Experimental Research on the Impact of Dielectric Characteristics on NO Removal by a Dielectric-barrier Discharge** [刊,汉] / YU Gang, GU Fan, XU Yi-qian, et al (Education Ministry Key Laboratory on Clean Coal Power Generation and Combustion Technology under the Southeastern University, Nanjing, China, Post Code: 210096) //Journal of Engineering for Thermal Energy &Power. — 2003, 18(5). —475～477

The impact of dielectric characteristics on NO removal is studied under the presence of dielectric-barrier discharge plasma. First, a NO removal test system with the use of the dielectric-barrier discharge plasma was set up. An experimental study was conducted of the NO removal efficiency by using various dielectrics, such as Al_2O_3, CaO, MgO and glass, etc. Then, a theoretical analysis was performed of the mechanism of such an impact. The results of experiment and theoretical analyses indicate that the electric field intensity of gas discharge formed by various barrier dielectrics are different with the energy provided to activated particles also being different. This results in a different influence on the NO removal rate. **Key words**: NO, dielectric-barrier discharge, dielectric constant, plasma

非对称渐开线直齿轮齿廓设计与有限元分析＝**Tooth Profile Design for and Finite Element Analysis of Asymmetrical Involute Spur Gears** [刊,汉] / JIANG Li-dong, CHANG Shan, SHI Yu-quan, et al (Harbin No. 703 Research Institute, Harbin, China, Post Code: 150036) //Journal of Engineering for Thermal Energy &Power. — 2003, 18(5). —478～481

Asymmetrical involute spur gears have different pressure angles on the drive side and coast side. A rational design of the tooth profile of such gears can lead to an increase in gear load capacity, a reduction in noise and vibration levels and a significant enhancement in bending strength. The authors have developed tooth-profile equations for the above-mentioned spur gears and relevant computer programs with calculation examples being given. In addition, a three-dimensional solid model of the spur gears was set up and a finite element analysis of the latter performed. **Key words**: asymmetrical involute spur gear, tooth profile design, finite element analysis

闭式内可逆中冷回热布雷顿循环的功率优化＝**Power Optimization of a Closed Brayton Cycle with Endo-reversible Intercooling and Regenerative Heating** [刊,汉] / WANG Wen-hua, CHEN Lin-gen, SUN Feng-rui (Department of Nuclear Energy Science and Engineering, Naval Engineering University, Wuhan, China, Post Code: 430033) //Journal of Engineering for Thermal Energy &Power. — 2003, 18(5). —482～485

The heat resistance losses of working mediums in high and low temperature-side heat exchangers, regenerative heaters and intercoolers have been taken into account for an endoreversible closed Brayton cycle under constant-temperature heat source conditions. With power output serving as an objective of optimization the authors have optimized the distribution of thermal conductivity values and intermediate pressure ratios for the above-mentioned items. Through the use of numerical calculations analyzed is the impact of several main cycle characteristic parameters on the distribution of maximum power, corresponding magnitudes of thermal conductivity, intermediate pressure ratios and the double maximum power. **Key words**: finite time thermodynamics, Brayton cycle, intercooling and regenerative heating, power optimization

光管和斜槽管降膜吸收数学模型及实验研究=**Mathematical Model for and Experimental Study of the Falling Film Absorption of Bare Tubes and Skewed-slot Low-ribbed Tubes** [刊, 汉] / WANG Mei-xia, ZHOU Qiang-tai (Power Engineering Department, Southeastern University, Nanjing, China, Post Code: 210096), LIU Cun-fang (College of Energy and Power Engineering, Shandong University, Jinan, China, Post Code: 250061) //Journal of Engineering for Thermal Energy & Power. — 2003, 18(5). —486 ~ 489

A mathematical model dealing with the falling film absorption of bare tubes and skewed-slot low-ribbed tubes has been set up. A numerical calculation method was used to solve for the outer layer model of bare tubes and skewed-slot low-ribbed tubes while an analytical method employed to solve for the velocity, temperature and concentration equation of the inner layer of the above-mentioned tubes. The calculated results were compared with those of tests, revealing a basic agreement between them with all errors being assessed at less than 10%. Causes leading to the errors were analyzed. It is concluded that the skewed-slot low-ribbed tubes can serve as intensification tubes suitable for use in absorption devices. **Key words**: skewed-slot low-ribbed tube, absorption, mathematical model, numerical calculation

热力学火用函数的基本微分关系与特征函数=**The Basic Differential Equations of Thermodynamics Exergy Function and Its Characteristic Functions** [刊, 汉] / HAN Guang-ze, WANG Xiao-wu, XIE Xin-an, et al (Department of Applied Physics, South China University of Science & Technology, Guangzhou, China, Post Code: 510640) // Journal of Engineering for Thermal Energy & Power. — 2003, 18(5). —490 ~ 492, 511

Proceeding from a universal expression of exergy, the authors have derived the first and second basic differential equations for the exergy function of a thermodynamics system. These two equations make it possible to change the exergy unfit for direct measurement into a function of measurable parameter. Through the use of basic differential relations the characteristics of system exergy function can be studied by experimental means. Moreover, it is also feasible to solve for the exergy function of a system. After a proper selection of free variables the exergy function of a system can serve as a characteristic function, from which all other thermodynamic functions may be determined. **Key words**: thermodynamics, exergy, basic differential equation, characteristic function

一种新型锅炉给水除氧器的研究=**A Study of a New Type of Boiler Feedwater Deaerator** [刊, 汉] / ZHANG Lin-hua (College of Environmental Engineering under the Xi'an University of Architectural Science & Technology, Xi'an, China, Post Code: 710055), CUI Yong-zhang, QU Yun-xia, et al (Department of Air Conditioning & Refrigeration Engineering, Shandong Institute of Architectural Engineering, Jinan, China, Post Code: 250014) //Journal of Engineering for Thermal Energy & Power. — 2003, 18(5). —493 ~ 496

The study results of an innovative boiler feedwater deaerator, which removes oxygen by a process of hydrogenation, are presented. Its operation principles and main components are described and compared with those of other deaeration methods. The factors affecting deaeration effectiveness are analyzed. Tests have shown that the hydrogenated deaerator features a stable and reliable operation and high deaeration effectiveness with the content of residual dissolved oxygen in the outgoing water fully complying with boiler feedwater quality standards. Such deaerators can be widely used in boiler feedwater systems and for supplying make-up water to hot water boilers and heat supply systems. **Key words**: deaeration, deaerator, catalysis, hydrogenation, dissolved oxygen

循环流化床锅炉 J 形返料阀的设计=**Design of a J-shaped Refeed Valve for a Circulating Fluidized Bed Boiler**